SPATIAL TRENDS IN MINERAL ABUNDANCES ACROSS TYRRHENA TERRA ON MARS. D. Tirsch[1], J.R.C. Voigt[2], C.E. Viviano[3], J.L. Bishop[4], M.D. Lane[5], L.L. Tornabene[6] and D. Loizeau[7]; [1]German Aerospace Center (DLR), Berlin, Germany (Daniela.tirsch@dlr.de); [2]Lunar and Planetary Laboratory, University of Arizona, Tucson, AZ; [3]Johns Hopkins University Applied Physics Lab, Laurel, MD; [4]SETI Institute, Mountain View, CA; [5]Fibernetics LLC, Lititz, PA; [6]University of Western Ontario (London, Canada); [7]Institut d'Astrophysique Spatiale, CNRS/Univ. Paris-Sud, France.

Introduction: Tyrrhena Terra (TT) hosts an intriguing variety of aqueously altered materials accompanied by unaltered mafic rocks. Our study region extends from the southern rim of the Isidis impact basin, including the Libya Montes region, southward to the Hellas Basin rim (Fig. 1). The NW part is dominated by lava flows from Syrtis Major that grade southwards into the TT highlands, dissected by fluvial channels and overprinted by abundant impact craters. These landforms together with lobate and fan-shaped deposits within impact craters are evidence for a variable history of erosion and deposition. Ancient phyllosilicate-rich materials have been exposed and uplifted from the subsurface, as they often occur in crater ejecta and central crater uplifts. Our previous studies used CRISM spectral data together with CTX, HiRISE, and HRSC images as well as their derived topography data to create geomorphological maps of the southern Isidis region and TT [1-5]. These datasets were used to map and characterize the types and occurrences of phyllosilicates, chlorite, opal, zeolites, carbonates, olivines, and pyroxenes and to assess the relationships between selected aqueous outcrops and surface features [1-5].

In this work, we build on these results by seeking correlations between aqueous mineral detections [1,2,4] with our geomorphological map [3] to assess 1) whether or not there are relationships between specific units and mineral occurrences, and 2) if there are trends across the study region in terms of mineral occurrence and abundance.

Methods: The geomorphological map introduced by Tirsch et al. [3] was extensively updated for this study. Unit names, unit assignments, and the extent of the mapped area were carefully revised; however, the color assignments and characteristics of the mapped units remain unchanged. Thus, we do not elaborate on the characteristics of the individual map units here but refer the interested reader to Tirsch et al. [3], with the exception of the new unit *crater floor* (cf) that includes all crater floor materials on which no other geomorphological unit defined here is identified. The map base is an HRSC nadir mosaic with 50 m/px spatial resolution and a mapping scale of 1:500,000 to comply with the large extent of the mapped region. The relative ages of the areal map units were estimated by means of crater-size-frequency-distributions derived from CTX image data. The resulting ages are displayed in the unit labels as N for Noachian, H for Hesperian, and A for Amazonian. The mineralogical map [4,6] spans not only the inter-Isidis-Hellas region, but also extends northwards to Nili Fosse and westwards to Terra Sabea. The focus of that study was on the metamorphic- and hydrothermally-related alteration history [4] using CRISM targeted and mapping data, including hundreds of calibrated MTRDR images. The mineral assemblages detected within our study region are listed in the legend of Fig. 1. These mineral detections [4] enabled us to assess the minerals in context with the geomorphological map. We utilized ESRI's ArcGIS software and conducted multiple statistical queries in terms of mineral occurrence/type versus geomorphological unit. In order to reveal possible trends across TT, we divided the study region into three spatial subregions: 1) a northern region covering the southern Isidis impact rim region, i.e., Libya Montes, as well as the southern tip of the Syrtis Major lava deposits, 2) a central region representing mostly the TT cratered highlands, and 3) a southern region comprising the distal region of the degraded Hellas Basin rim. This subdivision (marked as red lines in Fig. 1) is intended to reflect potentially different influences by the major impact events (i.e., Isidis and Hellas). The 21 datasets extracted by this method (7 map units x 3 geographical regions) were analyzed in Microsoft Excel. The pie charts visualizing the mineral abundances per individual mapping unit are shown in Fig. 1.

Limitations: We note that the different map scales of the two datasets (i.e., coarser scale geomorphological map (50 m/px) versus finer scale CRISM detections (18 m/px)) can induce biases in the results as the extent of a particular map unit (e.g., an ejecta blanket) is not always congruent with the extent of outcrops in the mineralogical map, enabling the potential for mineral detections to overlap geomorphological units. We minimized the influence of this discrepancy by considering only those mineral polygons whose centroid (i.e., the major part) lies within the queried map unit, while ignoring smaller overlaps into other units.

Results and Discussion: The results of this analysis are graphically summarized in Fig. 1. Ancient Noachian/Hesperian aged mountainous massif and crater rim materials (NHm) comprise the greatest variety of aqueous mineral assemblages, which are

dominated by Fe/Mg-phyllosilicates. The variety of these aqueous alteration minerals increase southwards, which might indicate that multiple processes acted on the region closer to Hellas. Furthermore, ancient and altered massif units could be well more exposed by the Hellas rim. However, the higher temperature products including chlorite/prehnite and zeolite are more abundant in the central region. The increased abundance of zeolite and high-temperature phyllosilicates in the central area is associated with a region of elevated groundwater from geothermal flux where hydrothermal activity is proposed [7]. Because we observe primarily Fe/Mg-smectite near Isidis (along with carbonate and Al-smectite detected at Libya Montes in earlier studies [1,2]) compared to a wider variety of aqueous materials near Hellas, the latter impact event likely triggered more long-term and varied aqueous responses than Isidis.

Fluvially dissected units of a similar age (NHf) are almost exclusively comprised of Fe/Mg-phyllosilicates. Inter-crater plains (NHicp) are likewise dominated by Fe/Mg-phyllosilicates, followed by chlorite/prehnite/epidote occurrences (~12%), which have their highest abundance within the central TT region. We interpret that this mineral variability is inherent to the NHicp unit, as it represents the extensive plains that group together all surfaces not assigned to other map units. Hesperian/Amazonian-aged ridged plains (HArp), which often represent volcanic deposits, contain Fe/Mg-phyllosilicates as well, but at a much lower abundance compared to the other units. The northern and central HArp materials are comprised of minor amounts of chloride/prehnite/epidote minerals, while zeolite is present in southern HArp materials. This trend also applies for the crater-related materials (cf and ej). A subjective visual contemplation of the mapped aqueous mineral occurrences indicates an association with crater-related materials. Our future studies will further investigate this relationship and refine associations of aqueous mineral types and abundances with geomorphological units, including the study of four fan-shaped and lobate deposits in our study region (fld) that show detections of Fe/Mg-phyllosilicates, compared to 16 other similar deposits that do not show such detections.

Conclusions: Fe/Mg-phyllosilicates are the dominant aqueous mineral type within the study region and are more abundant in the central region compared to the proximity of either the Isidis or Hellas impact basin. Chlorites increase in abundance with distance from both impact basins, which could be an indication of hydrothermal processes from geothermal flux. The large Hellas impact event appears to have produced more varied temperatures and water chemistries, resulting in increased mineral variability near its rim.

Acknowledgments: This work was supported by MDAP #80NSSC18K1384 (JLB, MDL, LLT).

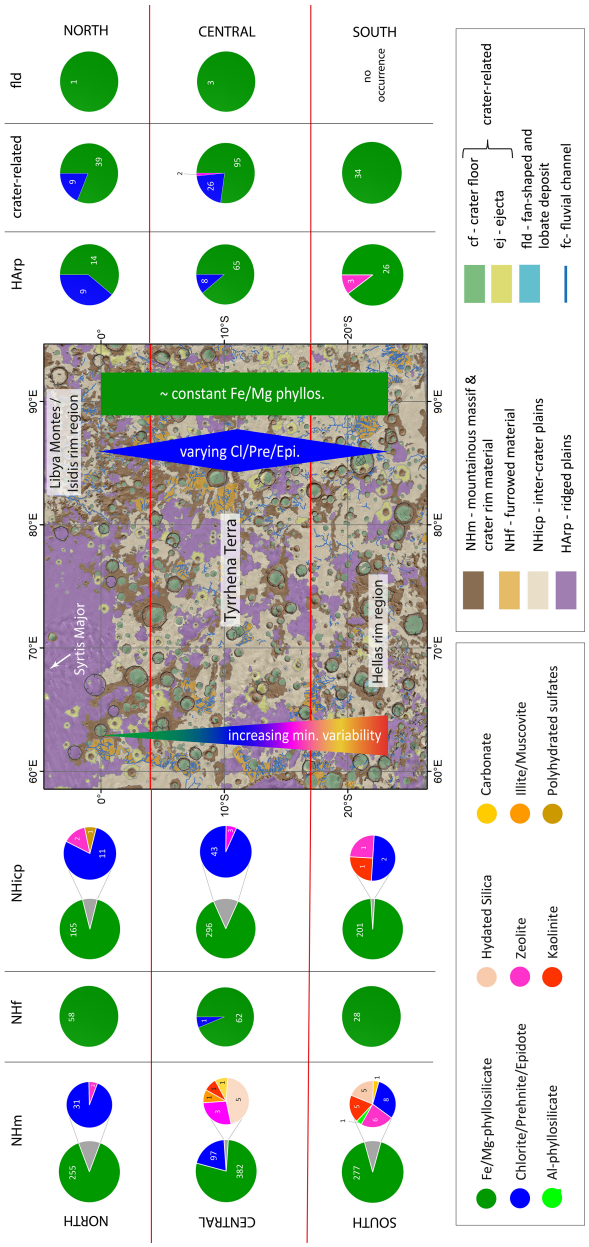

Fig. 1: Spatial distribution of aqueous minerals across Tyrrhena Terra shown by pie charts arranged around a geomorphological map. The pie charts refer to their respective subregions (divided by red lines) and mapping units (column headings). Graphics overlying the map show general trends across the entire region.

References: [1] Bishop J.L. et al. (2013) *JGR, 118*, 487–513. [2] Tirsch D. et al. (2018) *Icarus, 314*, 12-34. [3] Tirsch, D. et al. (2019) *50th LPSC*, Abstract #1532. [4] Viviano C.E. & Phillips M.S. (2019) *9th Conf. on Mars*, Abstract #6359. [5] Lane, M.D. et al. (2019) *9th Conf. on Mars*, Abstract #6422. [6] Viviano C.E. & Phillips M.S. (2019) *50th LPSC*, Abstract #2824. [7] Ojha L. et al. (2020) *Sci. Adv., 6 (49)*, eabb1669.